

# Supporting Information for A Versatile Strategy for Controlled Assembly of Plasmonic Metal/Semiconductor Hemispherical Nano-heterostructure Arrays

Meng Jia,<sup>†</sup> Yuying Zhang,<sup>‡</sup> Zhengxin Li,<sup>†</sup> Emma Crouch,<sup>†</sup> Samantha Doble,<sup>†</sup>  
Joseph Avenoso,<sup>¶</sup> Han Yan,<sup>†</sup> Chaoying Ni,<sup>‡</sup> and Lars Gundlach<sup>\*,†,¶</sup>

<sup>†</sup>*Department of Chemistry and Biochemistry, University of Delaware, Newark, Delaware,  
USA*

<sup>‡</sup>*Department of Material Science, University of Delaware, Newark, Delaware, USA*

<sup>¶</sup>*Department of Physics and Astronomy, University of Delaware, Newark, Delaware, USA*

E-mail: larsg@udel.edu

## 1 Experimental Details

### Fabrication of well-ordered metal nanoparticle array

Metal (Au and Ag) nanoparticle arrays were fabricated based on a physical vapor deposition process combined with nanosphere lithography (NSL). The monodisperse polystyrene (PS) spheres were purchased from Polyscience Inc. as suspensions in water (concentration of about 2.5 wt%) with a mean diameter of 500 nm. The suspension was used as received without any further filtration and dilution. The substrates used in this study were 100  $\mu\text{m}$ -thick microscope glass cover slide and fused silica (Alfa Aesar) with the size of 25  $\times$  25  $\text{mm}^2$  and

cleaned in hot piranha solution for 30 min. Prior to nanosphere deposition, the substrate was rinsed with deionized water, the sample was dried with N<sub>2</sub> and subsequently plasma cleaned (PDC-32G, Harrick Plasma) for 2 min to increase the hydrophilicity.

The spin coating of the PS nanosphere suspension onto the substrate was performed with a low-speed spin-coater (SCK-300S, Instras Scientific) following a three-step scheme: I. ramp the rotation speed to 100 RPM and slowly deposit 30  $\mu$ L suspension to the center of the substrate; II. gradually increase the rotation speed to 400 RPM in 30 seconds and spin for 2 min; III. further increase the rotation speed to 1000 RPM to fully dry the liquid.

After the formation of the nanosphere masks, a thin metal film with specific thickness (15 - 100 nm in this paper) was deposited on the nanosphere masks by thermal evaporation of metal in a vacuum chamber with a pressure of  $1 \times 10^{-5}$  Torr (dual e-beam evaporator, PVD Product Inc.). The metal film was deposited at a rate of  $\sim 1$   $\text{\AA}/\text{s}$ . The nanosphere masks were lifted off from the substrate by sonicating in toluene (Alfa Aesar, anhydrous, 99.8%), and the metal prisms were left on the surface of the substrate (**Fig. 2(b)**). Annealing the Au prism array at a temperature of 550°C leads to the formation of partially embedded Au nanoparticles (**Fig. 2c**). The annealing of the Ag nanoparticles was achieved at 300°C which was significantly lower than for Au nanoparticles

### **Synthesis of Cu<sub>2</sub>O semishell on metal nanoparticles**

Au/Cu<sub>2</sub>O and Ag/Cu<sub>2</sub>O nanostructure were prepared by chemical bath deposition and electrochemical deposition methods. The chemical bath deposition solution was prepared by adding 14 ml of deionized H<sub>2</sub>O, 200  $\mu$ L of 0.1 M copper(II) sulfate pentahydrate solution (ACS reagent, 98.0%), 0.1 mL 38.8mM sodium citrate solution (Na<sub>3</sub>C<sub>6</sub>H<sub>5</sub>O<sub>7</sub> · 2H<sub>2</sub>O, Thermo Fisher, 100%) and 0.087 g of sodium dodecyl sulfate (SDS, Fisher Scientific, 99%) in sequence to a beaker. Then, the substrate with the Au nanoparticle array was placed in the beaker. 300  $\mu$ L of 1M sodium hydroxide (NaOH, Alfa Aesar, 99 %) solution and 100  $\mu$ L of 0.2 M hydroxylamine hydrochloride (NH<sub>2</sub>OH·HCl, Sigma-Aldrich, 99%) were slowly added to the

solution in sequence under magnetic stirring. After one hour under room temperature, the substrate was taken out and rinsed with DI water for several times to get rid of impurities and surfactant. Heterostructures with thicker  $\text{Cu}_2\text{O}$  semishell (25 and 60 nm) was prepared by increasing the growth time and concentration of the copper salt solution.

The electrochemical deposition was conducted with a potentiostat (Bio-logic Science Instruments, SP-200) at constant voltage of -0.5 V vs. Ag/AgCl (sat. KCl). The working electrode was the Au nanoparticle arrays on the glass substrate. The counter electrode was a platinum wire. Ag/AgCl immersed in saturated KCl solution was used as the reference electrode.

The copper alkaline solution was prepared from 0.6 M  $\text{Cu}^{2+}$  and 3 M lactate acid from copper(II) sulfate pentahydrate (ACS reagent, 98.0%) added into lactic acid (Fisher Scientific, 99%) and then stirred with 5 M NaOH (Alfa Aesar, 99 %) solution to obtain a stable solution. The lactic acid was added as a buffer to keep  $\text{Cu}^{2+}$  soluble at the chosen pH. The stirred solution was then adjusted by addition of NaOH solution to a  $\text{pH} \approx 10.0$ . The duration for deposition was 1 hour at  $50^\circ\text{C}$ . The deposit was cleaned with deionized water to remove the remaining impurities. The sample were then dried at room temperature and the following analysis was performed.

## Characterizations

The morphologies of the materials were characterized by a ZEISS Auriga 60 scanning electron microscope (SEM) equipped with an energy dispersive X-ray spectroscopy detector (EDS) and a Talos F200C transmission electron microscope (TEM). UV-Vis absorption measurements were carried out with a photon control fiber spectrometer (SPM-002, Photon Control Inc.). The phase structure was determined by using a Bruker D8 X-ray diffraction (XRD) instrument with  $\text{Cu K}\alpha$  radiation. The elemental compositions were measured with a Thermo Fisher K-Alpha X-ray photoelectron spectrometer (XPS) with an Al  $\text{K}\alpha$  X-ray source at an energy of 1486.6 eV at base pressure below  $5 \times 10^{-8}$  Torr. The high resolution

spectra for Cu 2p, Cu LMM and Au 4f were collected with the pass energy of 20 eV. The data analysis was performed with the Aventura (version 5.9913) software. All peak positions and relative sensitivity factors were calibrated to the C 1s peak at 285 eV.

**Size distribution Calculation** Particle size distributions were calculated from SEM results with the ImageJ (version 1.52a) program. In **Figure 3**, the size distributions of Au NP and Au/Cu<sub>2</sub>O heterostructure arrays were compared as histograms.

## 2 Supporting Figures

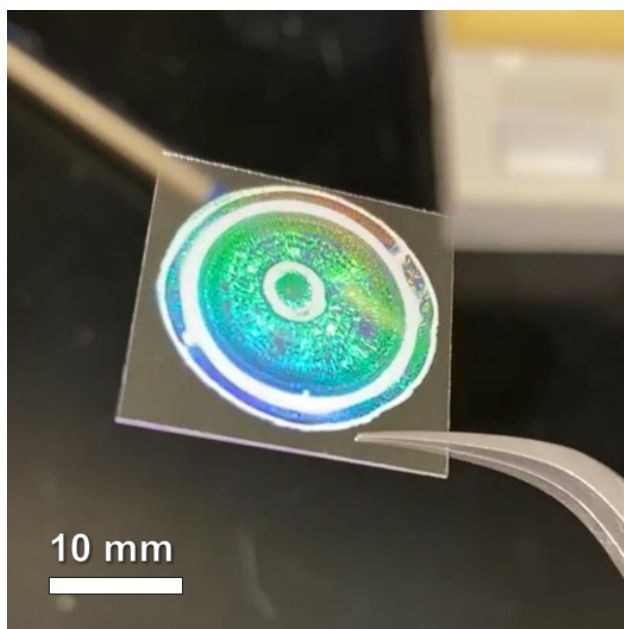


Figure S1: Photo of PS sphere monolayer mask on the glass substrate prepared through spin coating method.

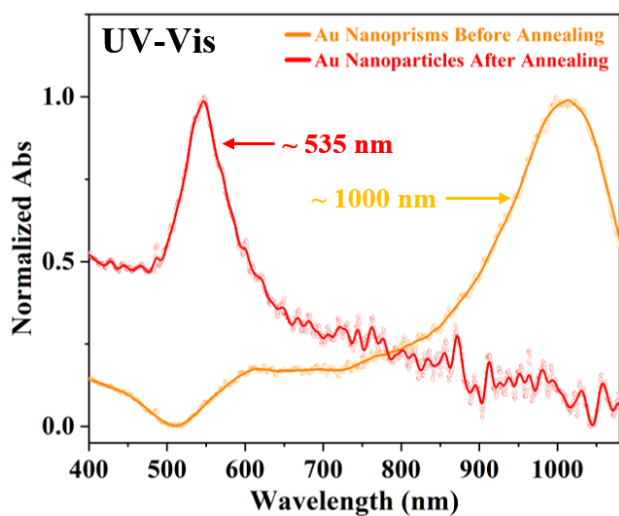


Figure S2: UV-Vis spectra of triangular Au nanoprism (orange) and Au nanohemisphere (Red) arrays after annealing.

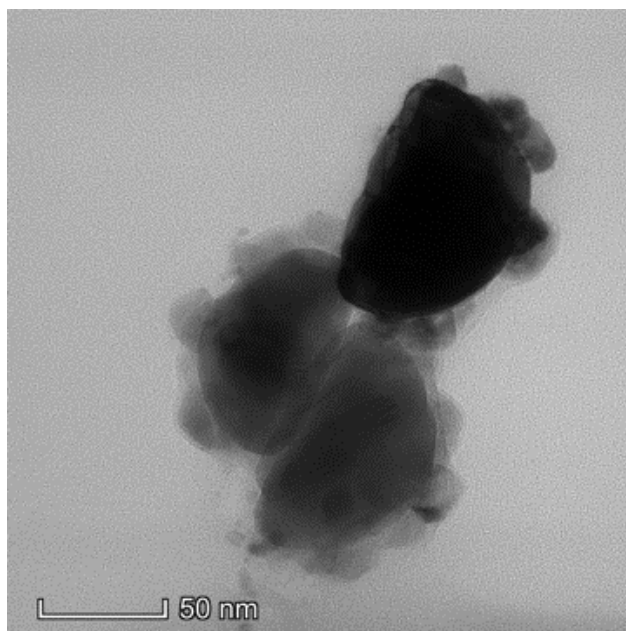


Figure S3: TEM image of the side view of Au/Cu<sub>2</sub>O heterostructures. A hemispherical shape of the metal core can be clearly observed for the right-top heterostructures. The samples were prepared by scratching off the heterostructures from the substrate. The heterostructures were collected in methanol then deposited onto a TEM grid. Therefore, some aggregation between these heterostructures as shown in this image are normal during the TEM sample preparation process.

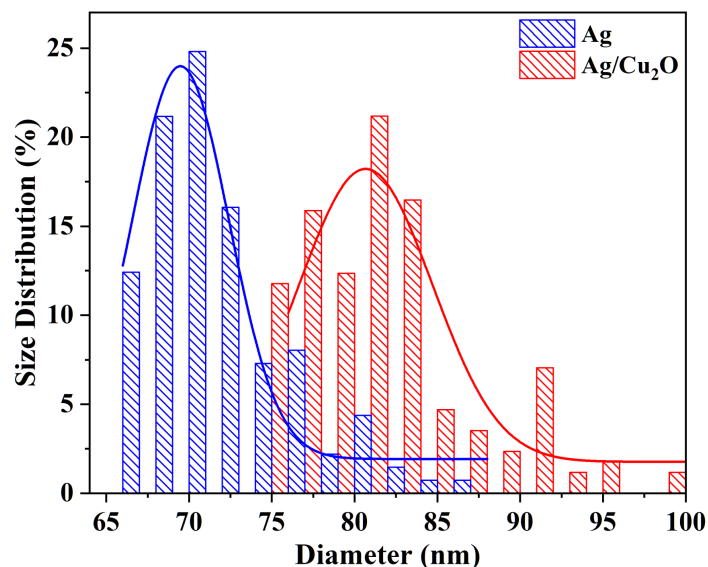


Figure S4: Histograms of size distribution of Ag nanoparticles (blue) and Ag/Cu<sub>2</sub>O heterostructures (red) with the corresponding Gaussian fits.

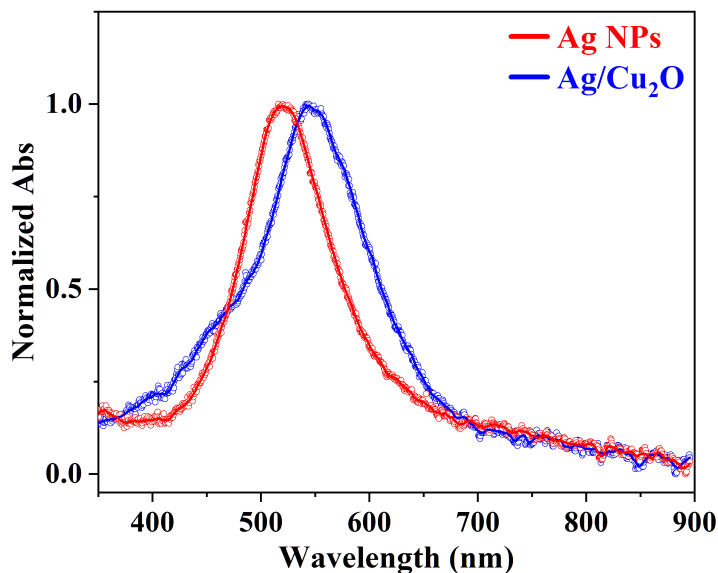


Figure S5: UV-Vis spectra of Ag nanoparticle (red) and Ag/Cu<sub>2</sub>O heterostructure (blue) arrays. The LSPR absorption position of Ag nanoparticles is observed at 520 nm. The red shifted absorption maximum with respect to the literature value (450 nm<sup>1</sup>) is attributed to its ellipsoidal shape (Figure 7). A similar red-shift tendency has been observed for Au nanoparticles from 550 nm (annealing at 500 °C) to 620 nm (annealing at 300 °C).<sup>2</sup>

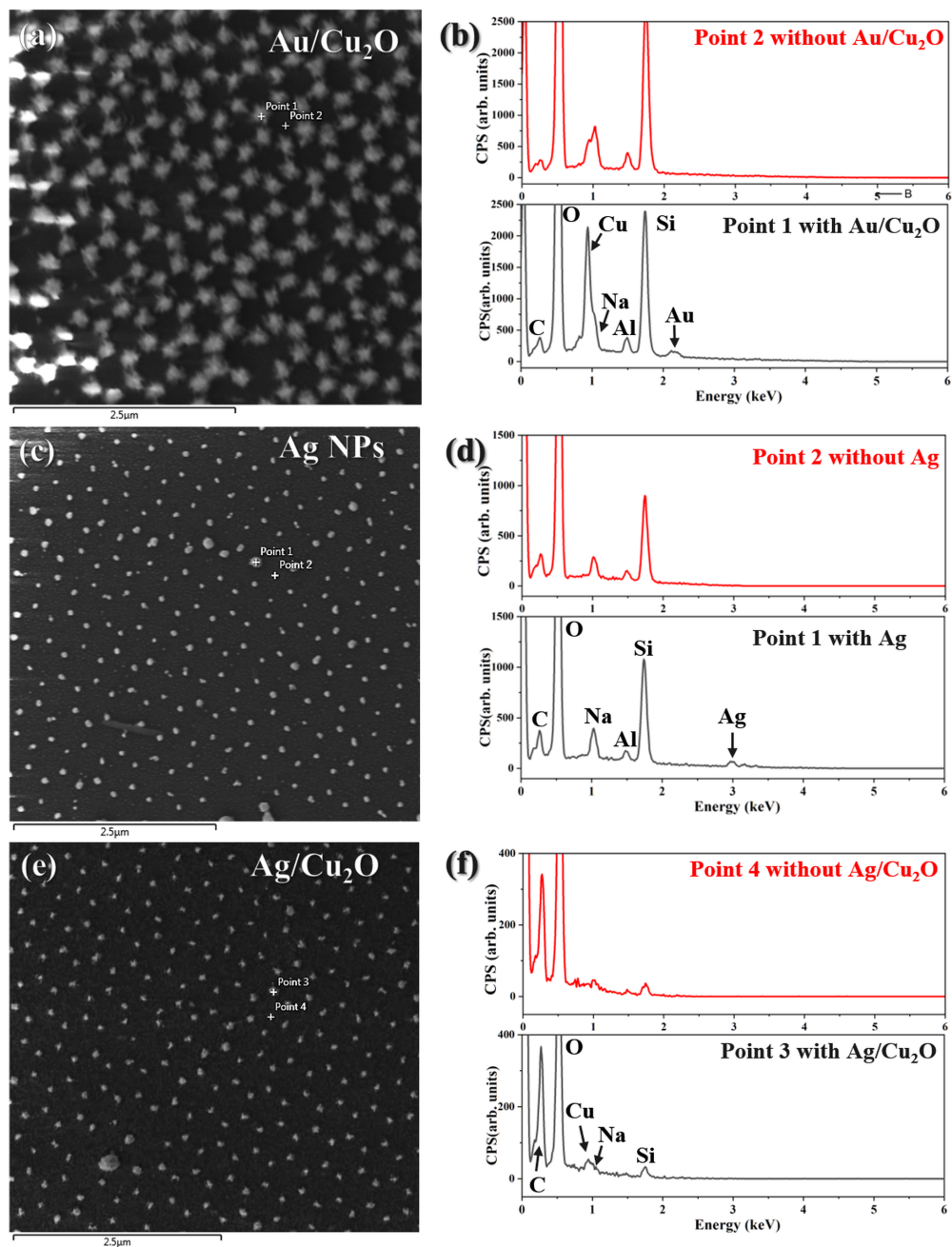


Figure S6: SEM-EDS measurements for the Au/Cu<sub>2</sub>O heterostructures (a,b), Ag nanoparticles (c,d), and Ag/Cu<sub>2</sub>O heterostructures (e,f). The EDS spectra compared the elemental composition between the spots with a single heterostructure and without any feature. The Si and Al peaks are attributed to the glass substrate. The Na signal is attributed to the sodium citrate salt from the solution-based chemical deposition process. The Au/Cu<sub>2</sub>O sample (a) corresponds to Au nanoparticles with  $\sim 71$  nm diameter and  $\sim 60$  nm Cu<sub>2</sub>O thickness. The sample of Ag nanoparticles (c) have a diameter of  $\sim 70$  nm. Ag/Cu<sub>2</sub>O samples (e) corresponds to Ag nanoparticles with  $\sim 70$  nm diameter and semishell with  $\sim 10$  nm Cu<sub>2</sub>O thickness.

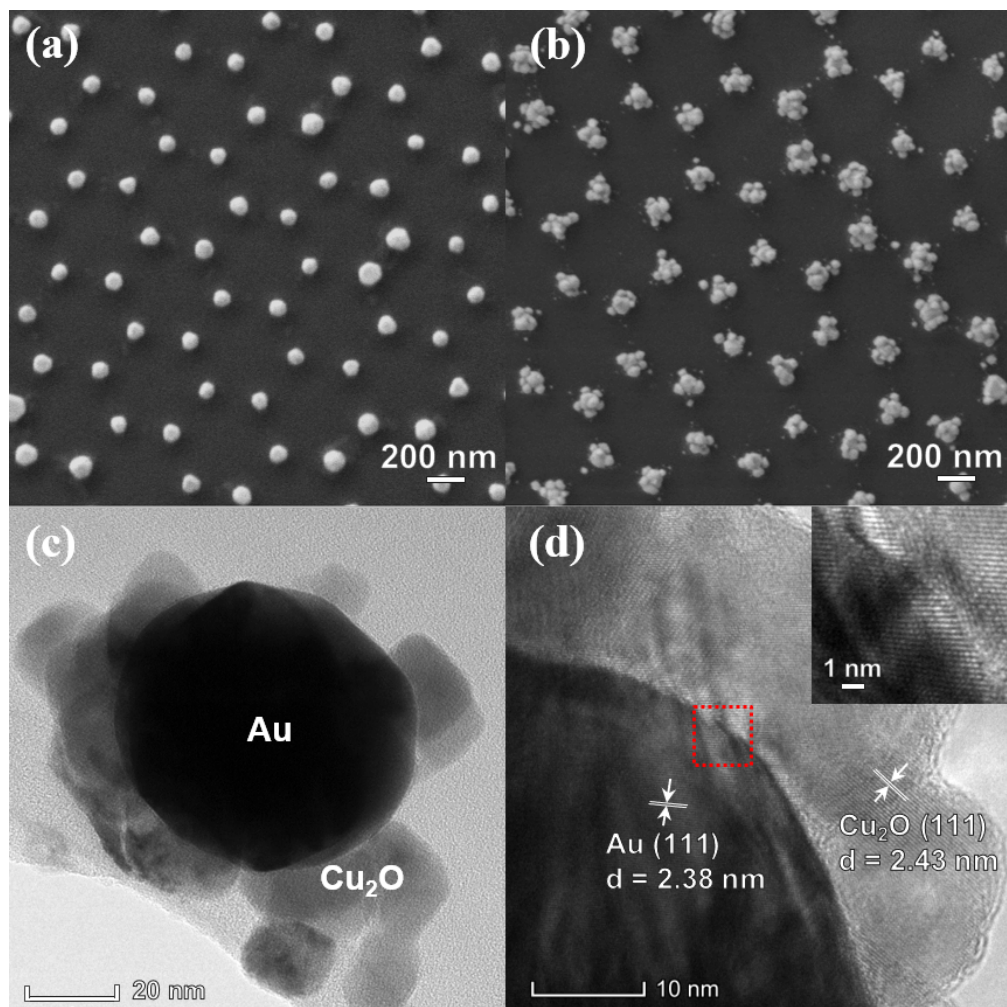


Figure S7: SEM images of (a) annealed Au nanoparticles and (b) Au/Cu<sub>2</sub>O heterostructure arrays on a fused silica substrate; TEM image of (c) a single Au/Cu<sub>2</sub>O heterostructure and (d) HR-TEM image of the cross-section of Au/Cu<sub>2</sub>O interface. A thicker semishell (~ 18 nm) was achieved by increasing the deposition time to two hours. Note: the deposition of Cu<sub>2</sub>O was performed without stirring. Due to the poor dispersion of the solution, the surface of the Au nanoparticles were unevenly covered.



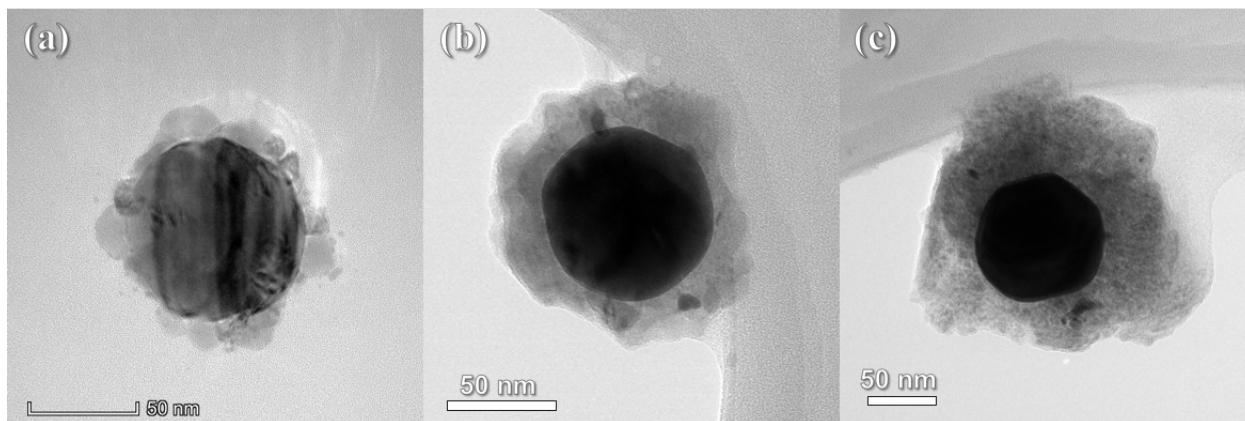


Figure S8: TEM images of Au/Cu<sub>2</sub>O heterostructures with the same Au core diameter with increasing Cu<sub>2</sub>O semishell thickness of ~10 nm (a), ~25 nm (b) and ~60 nm (c), respectively. (a) and (b) has been presented in the Fig. 2e and Fig. 6b.

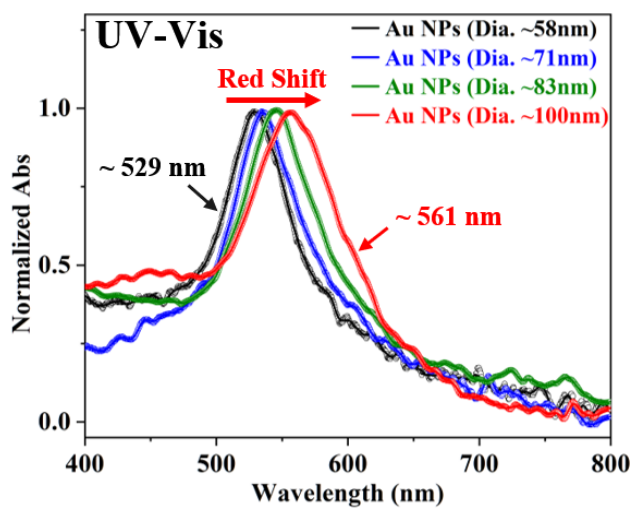


Figure S9: Tunable plasmonic properties of Au nanoparticles fabricated through NSL technique. UV-Vis spectra of Au nanoparticle arrays with different diameter of 58 (black), 71 (blue), 83 (green) and 100 nm (red).

## References

- (1) Paramelle, D.; Sadovoy, A.; Gorelik, S.; Free, P.; Hobley, J.; Fernig, D. G. A rapid method to estimate the concentration of citrate capped silver nanoparticles from UV-visible light spectra. *Analyst* **2014**, *139*, 4855–4861.
- (2) Colombelli, A.; Lospinoso, D.; Taurino, A.; Manera, M. G. Tailoring a periodic metal nanoantenna array using low cost template-assisted lithography. *Journal of Materials Chemistry C* **2019**, *7*, 13818–13828.